

Count-Based Exploration with the Successor Representation

Marlos C. Machado¹ Marc G. Bellemare² Michael Bowling^{1,3}

Abstract

In this paper we introduce a simple approach for exploration in reinforcement learning (RL) that allows us to develop theoretically justified algorithms in the tabular case but that is also extendable to settings where function approximation is required. Our approach is based on the successor representation (SR), which was originally introduced as a representation defining state generalization by the similarity of successor states. Here we show that the norm of the SR, while it is being learned, can be used as a reward bonus to incentivize exploration. In order to better understand this transient behavior of the norm of the SR we introduce the substochastic successor representation (SSR) and we show that it implicitly counts the number of times each state (or feature) has been observed. We use this result to introduce an algorithm that performs as well as some theoretically sample-efficient approaches. Finally, we extend these ideas to a deep RL algorithm and show that it achieves state-of-the-art performance in Atari 2600 games.

1. Introduction

Reinforcement learning (RL) tackles sequential decision making problems by formulating them as tasks where an agent must learn how to act optimally through trial and error interactions with the environment. The goal in these problems is to maximize the discounted sum of the numerical reward signal observed at each time step. Because the actions taken by the agent influence not just the immediate reward but also the states and associated rewards in the future, sequential decision making problems require agents to deal with the trade-off between immediate and delayed rewards. Here we focus on the problem of exploration in RL, which aims to reduce the number of samples (i.e., inter-

actions) an agent needs in order to learn to perform well in these tasks when the environment is initially unknown.

Surprisingly, the most common approach in the field is to select exploratory actions uniformly at random, with even high-profile success stories being obtained with this strategy (e.g., Tesauro, 1995; Mnih et al., 2015). However, random exploration often fails in environments with sparse rewards, that is, environments where the agent observes a reward signal of value zero for the majority of states.¹ In this paper we introduce a novel approach for exploration in RL based on the successor representation (SR; Dayan, 1993). The SR is a representation that generalizes between states using the similarity between their successors, that is, the states that follow the current state given the agent’s policy. The SR is defined for any problem, it can be learned with temporal-difference (TD) learning (Sutton, 1988) and, as we discuss below, it can be seen as implicitly estimating the transition dynamics of the environment.

The main contribution of this paper is to show that *the norm of the SR can be used as an exploration bonus*. We perform an extensive empirical evaluation to demonstrate this and we introduce the substochastic successor representation (SSR) to also understand, theoretically, the behavior of such bonus. The SSR behaves similarly to the SR but it is more amenable to theoretical analyses. We show that the SSR implicitly counts state visitation, suggesting that the exploration bonus obtained from the SR, while it is being learned, might also be incorporating some notion of state visitation counts. Finally, we extend the idea of using the norm of the SR as an exploration bonus to the function approximation case, designing a deep RL algorithm that achieves state-of-the-art performance in hard exploration Atari 2600 games when in a low sample-complexity regime. Importantly, the proposed algorithm is also simpler than traditional baselines such as pseudo-count-based methods as it does not require domain-specific density models (Bellemare et al., 2016; Ostrovski et al., 2017).

¹When we refer to environments with sparse rewards we do so for brevity and ease of presentation. Actually, any sequential decision making problem has dense rewards. In the RL formulation a reward signal is observed at every time step. By environments with sparse rewards we mean environments where the vast majority of transitions lead to reward signals with the same value.

¹Department of Computing Science, University of Alberta, Edmonton, AB, Canada ²Google Brain, Montréal, QC, Canada ³DeepMind Alberta, Edmonton, AB, Canada. Correspondence to: Marlos C. Machado <machado@ualberta.ca>.

2. Preliminaries

We consider an agent interacting with its environment in a sequential manner. Starting from a state $S_0 \in \mathcal{S}$, at each step the agent takes an action $A_t \in \mathcal{A}$, to which the environment responds with a state $S_{t+1} \in \mathcal{S}$ according to a transition probability function $p(s'|s, a) = \Pr(S_{t+1} = s' | S_t = s, A_t = a)$, and with a reward signal $R_{t+1} \in \mathbb{R}$, where $r(s, a)$ indicates the expected reward for a transition from state s under action a , i.e., $r(s, a) \doteq \mathbb{E}[R_t | S_t = s, A_t = a]$.

The value of a state s when following a policy π , $v_\pi(s)$, is defined to be the expected sum of discounted rewards from that state: $v_\pi(s) \doteq \mathbb{E}_\pi \left[\sum_{k=t+1}^T \gamma^{k-t-1} R_k \middle| S_t = s \right]$, with γ being the discount factor. When the transition probability function p and the reward function r are known, we can compute $v_\pi(s)$ recursively by solving the system of equations below (Bellman, 1957):

$$v_\pi(s) = \sum_a \pi(a|s) \left[r(s, a) + \gamma \sum_{s'} p(s'|s, a) v_\pi(s') \right].$$

These equations can also be written in matrix form with \mathbf{v}_π , $\mathbf{r} \in \mathbb{R}^{|\mathcal{S}|}$ and $P_\pi \in \mathbb{R}^{|\mathcal{S}| \times |\mathcal{S}|}$:

$$\mathbf{v}_\pi = \mathbf{r} + \gamma P_\pi \mathbf{v}_\pi = (I - \gamma P_\pi)^{-1} \mathbf{r}, \quad (1)$$

where P_π is the state to state transition probability function induced by π , that is, $P_\pi(s, s') = \sum_a \pi(a|s) p(s'|s, a)$.

Traditional model-based algorithms work by learning estimates of the matrix P_π and of the vector \mathbf{r} and using them to estimate \mathbf{v}_π , for example by solving Equation 1. We use \hat{P}_π and $\hat{\mathbf{r}}$ to denote empirical estimates of P_π and \mathbf{r} . Formally,

$$\hat{P}_\pi(s'|s) = \frac{n(s, s')}{n(s)}, \quad \hat{\mathbf{r}}(s) = \frac{C(s, s')}{n(s)}, \quad (2)$$

where $\hat{\mathbf{r}}(i)$ denotes the i -th entry in the vector $\hat{\mathbf{r}}$, $n(s, s')$ is the number of times the transition $s \rightarrow s'$ was observed, $n(s) = \sum_{s' \in \mathcal{S}} n(s, s')$, and $C(s, s')$ is the sum of the rewards associated with the $n(s, s')$ transitions (we drop the action to simplify notation). However, model-based approaches are rarely successful in problems with large state spaces due to the difficulty in learning accurate models.

Because of the challenges in model learning, model-free solutions largely dominate the literature. In model-free RL, instead of estimating P_π and \mathbf{r} we estimate $v_\pi(s)$ directly from samples. We often use TD learning (Sutton, 1988) to update our estimates of $v_\pi(s)$, $\hat{v}(s)$, online:

$$\hat{v}(S_t) \leftarrow \hat{v}(S_t) + \alpha [R_{t+1} + \gamma \hat{v}(S_{t+1}) - \hat{v}(S_t)], \quad (3)$$

where α is the step-size parameter. Generalization is required in problems with large state spaces, where it is unfeasible to learn an individual value for each state. We do so by parametrizing $\hat{v}(s)$ with a set of weights θ . We write, given

the weights θ , $\hat{v}(s; \theta) \approx v_\pi(s)$ and $\hat{q}(s, a; \theta) \approx q_\pi(s, a)$, where $q_\pi(s, a) = r(s, a) + \gamma \sum_{s'} p(s'|s, a) v_\pi(s')$. Model-free methods have performed well in problems with large state spaces, mainly due to the use of neural networks as function approximators (e.g., Mnih et al., 2015).

The ideas presented here are based on the successor representation (SR; Dayan, 1993). The successor representation with respect to a policy π , Ψ_π , is defined as

$$\Psi_\pi(s, s') = \mathbb{E}_{\pi, p} \left[\sum_{t=0}^{\infty} \gamma^t \mathbb{I}\{S_t = s'\} \middle| S_0 = s \right],$$

where we assume the sum is convergent with \mathbb{I} denoting the indicator function. This expectation can actually be estimated from samples with TD learning:

$$\hat{\Psi}(S_t, j) \leftarrow \hat{\Psi}(S_t, j) + \eta \left(\mathbb{I}\{S_t = j\} + \gamma \hat{\Psi}(S_{t+1}, j) - \hat{\Psi}(S_t, j) \right), \quad (4)$$

for all $j \in \mathcal{S}$ and η denoting the step-size. The SR also corresponds to the Neumann series of γP_π :

$$\Psi_\pi = \sum_{t=0}^{\infty} (\gamma P_\pi)^t = (I - \gamma P_\pi)^{-1}. \quad (5)$$

Notice that the SR is part of the solution when computing a value function: $\mathbf{v}_\pi = \Psi_\pi \mathbf{r}$ (Eq. 1). We use $\hat{\Psi}_\pi$ to denote the SR computed through \hat{P}_π , the approximation of P_π .

The definition of the SR can also be extended to features. Successor features (Barreto et al., 2017) generalize the successor representation to the function approximation setting. We use the definition for the uncontrolled case in this paper. Successor features can also be learned with TD learning.

Definition 2.1 (Successor Features). *For a given $0 \leq \gamma < 1$, policy π , and for a feature representation $\phi(s) \in \mathbb{R}^d$, the successor features for a state s are:*

$$\psi_\pi(s) = \mathbb{E}_{\pi, p} \left[\sum_{t=0}^{\infty} \gamma^t \phi(S_t) \middle| S_0 = s \right].$$

Alternatively, in matrix form, we can write the successor features as $\Psi_\pi = \sum_{t=0}^{\infty} (\gamma P_\pi)^t \Phi = (I - \gamma P_\pi)^{-1} \Phi$, where $\Phi \in \mathbb{R}^{|\mathcal{S}| \times d}$ is a matrix encoding the feature representation of each state such that $\phi(s) \in \mathbb{R}^d$. This definition reduces to the SR in the tabular case, where $\Phi = I$.

3. $\|\Psi(s)\|$ as an Exploration Bonus

It is now well-known that the SR incorporates diffusion properties of the environment (e.g., Machado et al., 2018b; Wu et al., 2019). These properties can be used to accelerate learning, for example, with options that promote exploration (Machado et al., 2018b). Inspired by these results, in

this section we argue that the SR can be used in a more direct way to promote exploration. We show that the norm of the SR, while it is being learned, behaves as an exploration bonus that rewards agents for visiting states it has visited less often. We first demonstrate this behavior empirically, in the tabular case, to clearly present the idea behind the introduced algorithm. We then introduce the substochastic successor representation in order to provide some theoretical intuition that justifies this idea. Later we show how these ideas carry over to the function approximation setting.

3.1. Empirical Demonstration

To demonstrate the usefulness of the norm of the SR as an exploration bonus we compare the performance of traditional Sarsa (Rummery & Niranjan, 1994) to Sarsa+SR, which incorporates the norm of the SR as an exploration bonus in the Sarsa update. The update equation for Sarsa+SR is

$$\hat{q}(S_t, A_t) \leftarrow \hat{q}(S_t, A_t) + \alpha \left(R_t + \beta \frac{1}{\|\hat{\Psi}(S_t)\|_1} + \gamma \hat{q}(S_{t+1}, A_{t+1}) - \hat{q}(S_t, A_t) \right), \quad (6)$$

where β is a scaling factor and, at each time step t , $\hat{\Psi}(S_t, \cdot)$ is updated before $\hat{q}(S_t, A_t)$ as per Equation 4.

We evaluated this algorithm in RiverSwim and SixArms (Strehl & Littman, 2008), traditional domains in the PAC-MDP literature that are used to evaluate provably sample-efficient algorithms. In these domains it is very likely that an agent will first observe a small reward generated in a state that is easy to get to. If the agent does not have a good exploration policy it is likely to converge to a suboptimal behavior, never observing larger rewards available in states that are difficult to get to.

Our results suggest that the proposed exploration bonus has a profound impact in the algorithm’s performance. When evaluating the agent for 5,000 time steps, Sarsa obtains an average return of approximately 26,000, while Sarsa+SR obtains an approximate average return of 1.8 million! Notice that, in RIVERSWIM, the reward that is “easy to get” has value 5, implying that, different from Sarsa+SR, Sarsa almost never explores the state space well enough. In SIXARMS the trend is the same. Sarsa obtains an approximate average return of 284,000 while Sarsa+SR achieves approximately 2.2 million. The actual numbers, which were averaged over 100 runs, are available in Table 1. Details about parameters as well as the empirical methodology are available in the Appendix.

3.2. Theoretical Justification

It is difficult to characterize the behavior of our proposed exploration bonus because it is updated at each time step with TD learning. It is hard to analyze the behavior of

Table 1. Comparison between Sarsa and Sarsa+SR. A 95% confidence interval is reported between parentheses.

	Sarsa	Sarsa + SR
RIVERSWIM	26,526 (2,350)	1,792,126 (258,709)
SIXARMS	284,013 (88,511)	2,176,044 (449,962)

estimates obtained with TD learning in the interim. Also, at its fixed point, the ℓ_1 -norm of the SR is $\sum \gamma^t 1 = 1/(1 - \gamma)$ for all states, making it hard for us to use the fixed point of the SR to theoretically analyze the behavior of this exploration bonus. In this section we introduce the substochastic successor representation (SSR) to provide some theoretical intuition of why the norm of the SR is a good exploration bonus. The SSR behaves similarly to the SR but it is simpler to analyze.

Definition 3.1 (Substochastic Successor Representation). *Let \tilde{P}_π denote the substochastic matrix induced by the environment’s dynamics and by the policy π such that $\tilde{P}_\pi(s'|s) = \frac{n(s,s')}{n(s)+1}$. For a given $0 \leq \gamma < 1$, the substochastic successor representation, $\tilde{\Psi}_\pi$, is defined as:*

$$\tilde{\Psi}_\pi = \sum_{t=0}^{\infty} \gamma^t \tilde{P}_\pi^t = (I - \gamma \tilde{P}_\pi)^{-1}.$$

The SSR only differs from the empirical SR in its incorporation of an additional “phantom” transition from each state, making it underestimate the real SR. Through algebraic manipulation we show that the SSR allows us to recover an estimate of the visit counts, $n(s)$. This result provides some intuition of why the exploration bonus we propose in this paper performs so well, as exploration bonuses based on state visitation counts are known to generate proper exploration.

As aforementioned, the SSR behaves similarly to the SR. When computing the norm of the SR, while it is being learned with TD learning, it is as if a reward of 1 was observed at each time step.² Thus, there is little variance in the target, with the predictions slowly approaching the true value of the SR. If pessimistically initialized, as traditionally done, the estimates of the SR approach the target from below. In this sense, the number of times a prediction has been updated in a given state is a good proxy to estimate how far this prediction is from its final target. From the definition above we can see that the SSR have similar properties. It underestimates the true target but slowly approaches it, converging to the true SR in the limit. The SSR simplifies the analysis by not taking bootstrapping into consideration.

The theorem below formalizes the idea that the norm of the

²When estimating the SR with TD learning, in vector form, the clause $\mathbb{I}\{S_t = j\}$, from Equation 4, is always true for one of the states, that is, an entry in the vector representing the SR. Thus, it is as if a reward of 1 was observed at each time step.

Table 2. Comparison between ESSR, R-MAX, E³, and MBIE. The numbers reported for R-MAX, E³, and MBIE are an estimate from the histograms presented by Strehl & Littman (2008). ESSR’s performance is the average over 100 runs. A 95% confidence interval is reported between parentheses.

	E ³	R-MAX	MBIE	ESSR
RIVERSWIM	3,000,000	3,000,000	3,250,000	3,088,924 (± 57,584)
SIXARMS	1,800,000	2,800,000	9,250,000	7,327,222 (± 1,189,460)

SSR implicitly counts state visitation, shedding some light on why the exploration bonus we propose works so well.

Theorem 1. Let $n(s)$ denote the number of times state s has been visited and let $\tilde{\Psi}_\pi$ denote the substochastic successor representation as in Definition 3.1. For a given $0 \leq \gamma < 1$,

$$\frac{\gamma}{n(s) + 1} - \frac{\gamma^2}{1 - \gamma} \leq (1 + \gamma) - \|\tilde{\Psi}_\pi(s)\|_1 \leq \frac{\gamma}{n(s) + 1}.$$

Proof of Theorem 1. Let \hat{P}_π be the empirical transition matrix. We first rewrite \tilde{P}_π in terms of \hat{P}_π :

$$\begin{aligned} \tilde{P}_\pi(s, s') &= \frac{n(s, s')}{n(s) + 1} = \frac{n(s)}{n(s) + 1} \frac{n(s, s')}{n(s)} \\ &= \frac{n(s)}{n(s) + 1} \hat{P}_\pi(s, s') \\ &= \left(1 - \frac{1}{n(s) + 1}\right) \hat{P}_\pi(s, s'). \end{aligned}$$

This expression can also be written in matrix form: $\tilde{P}_\pi = (I - N)\hat{P}_\pi$, where $N \in \mathbb{R}^{|S| \times |S|}$ denotes the diagonal matrix of augmented inverse counts. Expanding $\tilde{\Psi}_\pi$ we have:

$$\tilde{\Psi}_\pi = \sum_{t=0}^{\gamma} (\gamma \tilde{P}_\pi)^t = I + \gamma \tilde{P}_\pi + \gamma^2 \tilde{P}_\pi^2 \tilde{\Psi}_\pi.$$

The top eigenvector of a stochastic matrix is the all-ones vector, $\mathbf{1}$ (Meyn & Tweedie, 2012), and it corresponds to the eigenvalue 1. Using this fact and the definition of \tilde{P}_π with respect to \hat{P}_π we have:

$$\begin{aligned} \tilde{\Psi}_\pi \mathbf{1} &= (I + \gamma(I - N)\hat{P}_\pi) \mathbf{1} + \gamma^2 \tilde{P}_\pi^2 \tilde{\Psi}_\pi \mathbf{1} \\ &= (I + \gamma)\mathbf{1} - \gamma N \mathbf{1} + \gamma^2 \tilde{P}_\pi^2 \tilde{\Psi}_\pi \mathbf{1}. \end{aligned} \quad (7)$$

We can now bound the term $\gamma^2 \tilde{P}_\pi^2 \tilde{\Psi}_\pi \mathbf{1}$ using the fact that $\mathbf{1}$ is also the top eigenvector of the successor representation and has eigenvalue $\frac{1}{1-\gamma}$ (Machado et al., 2018b):

$$0 \leq \gamma^2 \tilde{P}_\pi^2 \tilde{\Psi}_\pi \mathbf{1} \leq \frac{\gamma^2}{1 - \gamma} \mathbf{1}.$$

Plugging (7) into the definition of the SR we have (notice that $\Psi(s)\mathbf{1} = \|\Psi(s)\|_1$):

$$(1 + \gamma)\mathbf{1} - \tilde{\Psi}_\pi \mathbf{1} = \gamma N \mathbf{1} - \gamma^2 \tilde{P}_\pi^2 \tilde{\Psi}_\pi \mathbf{1} \leq \gamma N \mathbf{1}.$$

When we also use the other bound on the quadratic term we conclude that, for any state s ,

$$\frac{\gamma}{n(s) + 1} - \frac{\gamma^2}{1 - \gamma} \leq (1 + \gamma) - \|\tilde{\Psi}_\pi(s)\|_1 \leq \frac{\gamma}{n(s) + 1}.$$

□

In other words, the SSR, obtained after a slight change to the SR, can be used to recover state visitation counts. The intuition behind this result is that the phantom transition, represented by the +1 in the denominator of the SSR, serves as a proxy for the uncertainty about that state by underestimating the SR. This is due to the fact that $\sum_{s'} \tilde{P}_\pi(s, s')$ gets closer to 1 each time state s is visited.

As a sanity check, we used this result to implement a simple model-based algorithm that penalizes the agent for visiting commonly visited states with the exploration bonus $r_{\text{int}} = -\|\tilde{\Psi}_\pi(s)\|_1$. Thus, our agent actually maximizes $r(s, a) + \beta r_{\text{int}}(s)$, with β being a scaling parameter. The shift $(1 + \gamma)$ in the theorem has no effect in the agent’s policy because it is the same across all states. In this algorithm the agent updates its transition probability model and reward model through Equation 2 and its SSR estimate as in Definition 3.1.

Table 2 depicts the performance of this algorithm, dubbed ESSR, as well as the performance of some algorithms with polynomial sample-complexity bounds. The goal with this evaluation is not to outperform these algorithms, but to evaluate how well ESSR performs when compared to algorithms that explicitly keep visitation counts to promote exploration. ESSR performs as well as R-MAX (Brafman & Tennenholtz, 2002) and E³ (Kearns & Singh, 2002) on RiverSwim and it outperforms these algorithms on SixArms; while MBIE (Strehl & Littman, 2008), which explicitly estimates confidence intervals over the expected return in each state, outperforms ESSR in these domains. These results clearly show that ESSR performs, on average, similarly to other algorithms with PAC-MDP guarantees, suggesting that the norm of the SSR is a promising exploration bonus. Additional details about the algorithm and the experimental methodology are available in the Appendix.³

³The code used to generate these results is available at: https://github.com/mcmachado/count_based_exploration_sr.

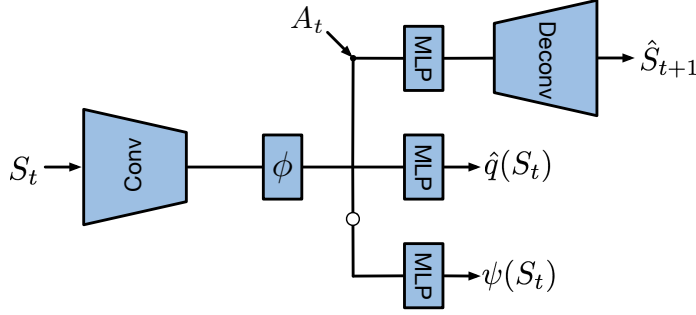


Figure 1. Neural network architecture used by our algorithm when learning to play Atari 2600 games.

4. Counting Feature Activations with the SR

In large environments, where enumerating all states is not an option, directly using Sarsa+SR as described in the previous section is not viable. Learning the SR becomes even more challenging when the representation, ϕ , is also being learned. Using neural networks to learn a representation while learning to estimate state-action value function is the approach that currently often leads to state-of-the-art performance in the field. In this section we describe an algorithm that uses the same ideas described so far but in the function approximation setting. Our algorithm was inspired by recent work that have shown that successor features can be learned jointly with the feature representation itself (Kulkarni et al., 2016; Machado et al., 2018b).

An overview of the neural network we used to learn the agent’s value function while also learning the feature representation and the SR is depicted in Figure 3. The layers used to compute the state-action value function, $\hat{q}(S_t, \cdot)$, are structured as in DQN (Mnih et al., 2015), but with different numbers of parameters (i.e., filter sizes, stride, and number of nodes). This was done to match Oh et al.’s (2015) architecture, which is known to succeed in the auxiliary task of predicting the agent’s next observation, which we detail below. From here on, we call the part of our architecture that predicts $\hat{q}(S_t, \cdot)$ DQN_e to distinguish between the parameters of this network and DQN. It is trained to minimize

$$\mathcal{L}_{\text{TD}} = \mathbb{E} \left[\left((1 - \tau) \delta(s, a) + \tau \delta_{\text{MC}}(s, a) \right)^2 \right],$$

with $\delta(s, a)$ and $\delta_{\text{MC}}(s, a)$ being defined as

$$\delta(s, a) = R_t + \beta r_{\text{int}}(s; \theta^-) + \gamma \max_{a'} q(s', a'; \theta^-) - q(s, a; \theta),$$

$$\delta_{\text{MC}}(s, a) = \sum_{t=0}^{\infty} \gamma^t \left(r(S_t, A_t) + \beta r_{\text{int}}(S_t; \theta^-) \right) - q(s, a; \theta).$$

This loss is known as the mixed Monte-Carlo return (MMC) and it has been used in the past by the algorithms that achieved successful exploration in deep reinforcement learning (Bellemare et al., 2016; Ostrovski et al., 2017). The

distinction between θ and θ^- is standard in the field, with θ^- denoting the parameters of the target network, which is updated less often for stability purposes (Mnih et al., 2015). As before, we use r_{int} to denote the exploration bonus obtained from the successor features of the internal representation, ϕ , which will be defined below. Moreover, to ensure all features are in the same range, we normalize the feature vector so that $\|\phi(\cdot)\|_2 = 1$. In Fig. 3 we highlight with ϕ the layer in which we normalize its output. Notice that the features are always non-negative due to the use of ReLU gates.

The successor features, $\psi(S_t)$, at the bottom of the diagram, are obtained by minimizing the loss

$$\mathcal{L}_{\text{SR}} = \mathbb{E}_{\pi, p} \left[\left(\phi(S_t; \theta^-) + \gamma \psi(S_{t+1}; \theta^-) - \psi(S_t; \theta) \right)^2 \right].$$

Zero is a fixed point for the SR, which is particularly concerning in settings with sparse rewards. The agent might end up learning to set $\phi(\cdot) = \vec{0}$ to achieve zero loss. We address this problem by not propagating $\nabla \mathcal{L}_{\text{SR}}$ to ϕ (this is depicted in Figure 3 as an open circle stopping the gradient); and by creating an auxiliary task (Jaderberg et al., 2017) to encourage a representation to be learned before a non-zero reward is observed. As Machado et al. (2018b), we use the auxiliary task of predicting the next observation, learned through the architecture proposed by Oh et al. (2015), which is depicted as the top layers in Figure 3. The loss we minimize for this last part of the network is

$$\mathcal{L}_{\text{Recons}} = (\hat{S}_{t+1} - S_{t+1})^2.$$

The overall loss minimized by the network is

$$\mathcal{L} = w_{\text{TD}} \mathcal{L}_{\text{TD}} + w_{\text{SR}} \mathcal{L}_{\text{SR}} + w_{\text{Recons}} \mathcal{L}_{\text{Recons}}.$$

The last step in describing our algorithm is to define $r_{\text{int}}(S_t; \theta^-)$, the intrinsic reward we use to encourage exploration. We choose the exploration bonus to be the inverse of the ℓ_2 -norm of the vector of successor features of the current state, as in Sarsa+SR. That is,

$$r_{\text{int}}(S_t; \theta^-) = \frac{1}{\|\psi(S_t; \theta^-)\|_2},$$

Table 3. Performance of the proposed algorithm, $\text{DQN}_e^{\text{MMC}} + \text{SR}$, compared to various agents on the “hard exploration” subset of Atari 2600 games. The DQN results reported are from Machado et al. (2018a) while the $\text{DQN}^{\text{MMC}} + \text{CTS}$ and $\text{DQN}^{\text{MMC}} + \text{PixelCNN}$ results were extracted from the learning curves available in Ostrovski et al.’s (2017) work and RND results were extracted from the learning curves available in Burda et al.’s (2019). $\text{DQN}_e^{\text{MMC}}$ denotes another baseline used in the comparison. When available, standard deviations are reported between parentheses. See text for details.

	DQN	$\text{DQN}_e^{\text{MMC}}$	$\text{DQN}^{\text{MMC}} + \text{CTS}$	$\text{DQN}^{\text{MMC}} + \text{PIXELCNN}$	RND	$\text{DQN}_e^{\text{MMC}} + \text{SR}$
FREEWAY	32.4 (0.3)	29.5 (0.1)	29.2	29.4	- -	29.5 (0.1)
GRAVITAR	118.5 (22.0)	1078.3 (254.1)	199.8	275.4	790.0 (122.9)	430.3 (109.4)
MONT. REV.	0.0 (0.0)	0.0 (0.0)	2941.9	1671.7	524.8 (314.0)	1778.6 (903.6)
PRIVATE EYE	1447.4 (2,567.9)	113.4 (42.3)	32.8	14386.0	61.3 (53.7)	99.1 (1.8)
SOLARIS	783.4 (55.3)	2244.6 (378.8)	1147.1	2279.4	1270.3 (291.0)	2155.7 (398.3)
VENTURE	4.4 (5.4)	1220.1 (51.0)	0.0	856.2	953.7 (167.3)	1241.8 (236.0)

where $\psi(S_t; \theta^-)$ denotes the successor features of state S_t parametrized by θ^- . The exploration bonus comes from the same intuition presented in the previous section (we observed in preliminary experiments not discussed here that DQN performs better when dealing with positive rewards). Moreover, we use the ℓ_2 -norm of the SR instead of the ℓ_1 -norm, which was used so far. This mismatch is further discussed in Section 5.3. It was driven by the ℓ_2 -norm leading to slightly better performance. A complete description of the network architecture is available in the Appendix.

5. Evaluation of Exploration in Deep RL

We evaluated our algorithm on the Arcade Learning Environment (Bellemare et al., 2013). Following Bellemare et al.’s (2016) taxonomy, we focused on the Atari 2600 games with sparse rewards that pose hard exploration problems. They are: FREEWAY, GRAVITAR, MONTEZUMA’S REVENGE, PRIVATE EYE, SOLARIS, and VENTURE.⁴

We used the evaluation protocol proposed by Machado et al. (2018a). We used MONTEZUMA’S REVENGE to tune our parameters. The reported results are the average over 10 seeds after 100 million frames. We evaluated our agents in the stochastic setting (sticky actions, $\varsigma = 0.25$) using a frame skip of 5 with the full action set ($|\mathcal{A}| = 18$). The agent learns from raw pixels i.e., it uses the game screen as input.

Our results were obtained with the algorithm described in Section 4. We set $\beta = 0.025$ after a rough sweep over values in the game MONTEZUMA’S REVENGE. We annealed ϵ in DQN’s ϵ -greedy exploration over the first million steps, starting at 1.0 and stopping at 0.1 as done by Bellemare et al. (2016). We trained the network with RMSprop with a step-size of 0.00025, an ϵ value of 0.01, and a decay of 0.95, which are the standard parameters for training DQN (Mnih et al., 2015). The discount factor, γ , is set to 0.99 and $w_{\text{TD}} = 1$, $w_{\text{SR}} = 1000$, $w_{\text{Recons}} = 0.001$. The weights w_{TD} , w_{SR} , and w_{Recons} were set so that the loss functions would be

roughly the same scale. All other parameters are the same as those used by Mnih et al. (2015).

5.1. Overall Performance and Baselines

Table 3 summarizes the results after 100 million frames. The performance of other algorithms is also provided for reference. Notice we are reporting *learning performance* for all algorithms instead of the maximum scores achieved by the algorithm. We use the superscript ^{MMC} to distinguish between the algorithms that use MMC from those that do not. When comparing our algorithm, $\text{DQN}_e^{\text{MMC}} + \text{SR}$, to DQN we can see how much our approach improves over the most traditional baseline. By comparing our algorithm’s performance to $\text{DQN}^{\text{MMC}} + \text{CTS}$ (Bellemare et al., 2016) and $\text{DQN}^{\text{MMC}} + \text{PixelCNN}$ (Ostrovski et al., 2017) we compare our algorithm to established baselines for exploration that are closer to our method. By comparing our algorithm’s performance to Random Network Distillation (RND; Burda et al., 2019) we compare our algorithm to the most recent paper in the field with state-of-the-art performance.

As mentioned in Section 4, the parameters of the network we used are different from those used in the traditional DQN network, so we also compared the performance of our algorithm to the performance of the same network our algorithm uses but without the additional modules (next state prediction and successor representation) by setting $w_{\text{SR}} = w_{\text{Recons}} = 0$ and without the intrinsic reward bonus by setting $\beta = 0.0$. The column labeled $\text{DQN}_e^{\text{MMC}}$ contains the results for this baseline. This comparison allows us to explicitly quantify the improvement provided by the proposed exploration bonus. The learning curves of these algorithms and their performance after different amounts of experience are available in the Appendix.

We can clearly see that our algorithm achieves scores much higher than those achieved by DQN, which struggles in games that pose hard exploration problems. Moreover, by comparing $\text{DQN}_e^{\text{MMC}} + \text{SR}$ to $\text{DQN}_e^{\text{MMC}}$ we can see that the provided exploration bonus has a big impact in the game MONTEZUMA’S REVENGE, which is probably known as

⁴The code used to generate these results is available at: https://github.com/mcmachado/count_based_exploration_sr.

the hardest game among those we used in our evaluation, and the only game where agents do not learn how to achieve scores greater than zero with random exploration. Interestingly, the change in architecture and the use of MMC leads to a big improvement in games such as GRAVITAR and VENTURE, which we cannot fully explain. However, notice that the change in architecture does not have any effect in MONTEZUMA’S REVENGE. The proposed exploration bonus seems to be essential in games with very sparse rewards. We also compared our algorithm to $\text{DQN}^{\text{MMC}}+\text{CTS}$ and $\text{DQN}^{\text{MMC}}+\text{PixelCNN}$. We can observe that, on average, $\text{DQN}_e^{\text{MMC}}+\text{SR}$ outperforms these algorithms while being simpler since it does not require a density model. Instead, our algorithm requires the SR, which is domain-independent as it is already defined for every problem since it is a component of the value function estimates, as discussed in Section 2.

Finally, $\text{DQN}_e^{\text{MMC}}+\text{SR}$ also outperforms RND (Burda et al., 2019) when it is trained for 100 million frames. Importantly, RND is currently considered to be the state-of-the-art approach for exploration in Atari 2600 games. Burda et al. did not evaluate RND in FREEWAY. Details about how the RND performance was obtained are available in the Appendix.

5.2. Evaluating the Impact of the Auxiliary Task

While the results depicted in Table 3 allow us to clearly see the benefit of using an exploration bonus derived from the SR, they do not inform us about the impact of the auxiliary task in the results. The experiments in this section aim at addressing this issue. We focus on MONTEZUMA’S REVENGE because it is the game where the problem of exploration is maximized, with most algorithms not being able to do anything without an exploration bonus.

The first question we asked was whether the *auxiliary task was necessary* in our algorithm. We evaluated this by dropping the reconstruction module from the network to test whether the initial random noise generated by the SR is enough to drive representation learning. It is not. When dropping the auxiliary task, the average performance of this baseline over 4 seeds in MONTEZUMA’S REVENGE after 100 million frames was 100 points ($\sigma^2 = 200$; min: 0, max: 400). As comparison, our algorithm obtains 1778.6 points ($\sigma^2 = 903.6$, min: 400, max: 2500). These results suggest that auxiliary tasks seem to be necessary for our method to perform well.

We also evaluated whether the *auxiliary task was sufficient* to generate the results we observed. To do so we dropped the SR module and set $\beta = 0.0$ to evaluate whether our exploration bonus was actually improving the agent’s performance or whether the auxiliary task was doing it. The exploration bonus seems to be essential. When dropping the exploration bonus and the SR module, the average performance of this baseline over 4 seeds in MONTEZUMA’S

Table 4. Performance of the proposed algorithm, $\text{DQN}_e^{\text{MMC}}+\text{SR}$, when using the ℓ_1 -norm and ℓ_2 -norm of the SR to generate the exploration bonus. Standard deviations are reported between parenthesis. See text for details.

	ℓ_1 -norm		ℓ_2 -norm	
FREEWAY	29.4	(0.1)	29.5	(0.1)
GRAVITAR	457.4	(120.3)	430.3	(109.4)
MONT. REV.	1395.4	(1121.8)	1778.6	(903.6)
PRIVATE EYE	104.4	(50.4)	99.1	(1.8)
SOLARIS	1890.1	(163.1)	2155.7	(398.3)
VENTURE	1348.5	(56.5)	1241.8	(236.0)

REVENGE after 100 million frames was 398.5 points ($\sigma^2 = 230.1$; min: 0, max: 400). Again, clearly, the auxiliary task is not a sufficient condition for the performance we report.

The reported results use the same parameters as before. Learning curves for each run are available in the Appendix.

5.3. On the Mismatch between the Used Norms

As aforementioned, there is a mismatch between theory and practice when looking at the deep RL algorithm we introduced in Section 4. While $\text{DQN}_e^{\text{MMC}}+\text{SR}$ uses the ℓ_2 -norm of the SR to generate the exploration bonus, our theoretical result is stated with respect to the ℓ_1 -norm of the SR. This mismatch was driven by the fact that, empirically, $\text{DQN}_e^{\text{MMC}}+\text{SR}$ exhibits a slightly better performance when using the ℓ_2 -norm of the SR instead of the ℓ_1 -norm. We conjecture this might be due to the fact that the ℓ_2 -norm is smoother than the ℓ_1 -norm, a property that is particularly important when training neural networks. Table 4 depicts a comparison between the performance of $\text{DQN}_e^{\text{MMC}}+\text{SR}$ when using the ℓ_2 -norm and the ℓ_1 -norm of the SR to generate its exploration bonus (ϕ is normalized with the respective norm).

We followed the same evaluation protocol described before, averaging the performance of $\text{DQN}_e^{\text{MMC}}+\text{SR}$ with the ℓ_1 -norm over 10 runs. The parameter β is the only parameter not shared by both algorithms. While $\beta = 0.025$ when using the ℓ_2 -norm of the SR, $\beta = 0.05$ when using the ℓ_1 -norm of the SR. These results also support the claim that the norm of the SR can be used to generate exploration bonuses. $\text{DQN}_e^{\text{MMC}}+\text{SR}$, when using the ℓ_1 -norm of the SR, exhibits performance comparable to pseudo-count based methods, despite not being the best results we obtained.

We also revisited the results presented in Section 3.1 to evaluate the impact of the different norms in Sarsa+SR. We swept over all the parameters, as previously described. The results reported for Sarsa+SR when using the ℓ_2 -norm of the SR are the average over 100 runs. The actual numbers are available in Table 5. The used parameters are discussed in the Appendix. Interestingly, we observe the same trend

Table 5. Performance of Sarsa+SR, in the tabular case, when using the ℓ_1 -norm and ℓ_2 -norm of the SR to generate the exploration bonus. A 95% confidence interval is reported between parentheses.

	ℓ_1 -norm	ℓ_2 -norm
RIVERSWIM	1,792,126 (258,709)	1,989,479 (167,189)
SIXARMS	2,176,044 (449,962)	2,625,132 (516,804)

we observed in the deep RL case. The ℓ_2 -norm of the SR leads to even better results.

The fact that the algorithms proposed in this paper perform better when using the ℓ_2 -norm of the SR instead of the ℓ_1 -norm deserves further investigation, either empirically or theoretically. We conjecture it might be possible to derive theoretical guarantees for the ℓ_2 -norm of the SR that are similar to those derived here. Nevertheless, these results suggest that the idea of using the norm of the SR for exploration is quite general, with the p -norm of the SR being effective for more than one value of p .

6. Related Work

There are multiple algorithms in the tabular, model-based case with guarantees about their performance in terms of regret bounds (e.g., Osband et al., 2016) or sample-complexity (e.g., Brafman & Tennenholtz, 2002; Kearns & Singh, 2002; Strehl & Littman, 2008). RiverSwim and SixArms are domains traditionally used when evaluating these algorithms. In this paper we have introduced a model-free algorithm that performs particularly well in these domains. We have also introduced a model-based algorithm that performs as well as some of these algorithms with theoretical guarantees. Among these algorithms, R-MAX seems the closest approach to ours. As with R-MAX, the algorithm we presented in Section 3.2 augments the state-space with an imaginary state and encourages the agent to visit that state, implicitly reducing the algorithm’s uncertainty in the state-space. However, R-MAX deletes the transition to this imaginary state once a state has been visited a given number of times. Ours, on the other hand, lets the probability of visiting this imaginary state vanish with additional visitations. Importantly, notice that it is not clear how to apply these traditional algorithms such as R-MAX and E^3 to large domains where function approximation is required.

Conversely, there are not many model-free approaches with proven sample-complexity bounds (e.g., Strehl et al., 2006), but there are multiple model-free algorithms for exploration that actually work in large domains (e.g., Stadie et al., 2015; Bellemare et al., 2016; Ostrovski et al., 2017; Plappert et al., 2018; Burda et al., 2019). Among these algorithms, the use of pseudo-counts through density models is the closest to ours (Bellemare et al., 2016; Ostrovski et al., 2017). Inspired by those papers we used the mixed Monte-Carlo return as a

target in the update rule. In Section 5 we have shown that our algorithm outperforms these approaches while being simpler by not requiring a density model. Importantly, Martin et al. (2017) had already shown that counting activations of fixed, handcrafted features in Atari 2600 games leads to good exploration behavior. Nevertheless, by using the SR we are not only counting *learned* features but we are also implicitly capturing the induced transition dynamics.

Finally, the SR has already been used in the context of exploration. However, it was used to help the agent learn how to act in a higher level of abstraction in order to navigate through the state space faster (Machado et al., 2018b). Such an approach has led to promising results in the tabular case but only anecdotal evidence about its scalability has been provided when the idea was applied to large domains such as Atari 2600 games. Importantly, the work developed by Machado et al. (2018b), Kulkarni et al. (2016) and Oh et al. (2015) are the main motivation for the neural network architecture presented here. Oh et al. (2015) have shown how one can predict the next screen given the current observation and action (our auxiliary task), while Machado et al. (2018b) and Kulkarni et al. (2016) have proposed different architectures for learning the SR from raw pixels.

7. Conclusion

RL algorithms tend to have high sample complexity, which often prevents them from being used in the real-world. Poor exploration strategies is one of the main reasons for this high sample-complexity. Despite all of its shortcomings, uniform random exploration is, to date, the most commonly used approach for exploration. This is mainly due to the fact that most approaches for tackling the exploration problem still rely on domain-specific knowledge (e.g., density models, handcrafted features), or on having an agent learn a perfect model of the environment. In this paper we introduced a general method for exploration in RL that implicitly counts state (or feature) visitation in order to guide the exploration process. It is compatible to representation learning and the idea can also be adapted to be applied to large domains.

This result opens up multiple possibilities for future work. Based on the results presented in Section 3.2, for example, we conjecture that the substochastic successor representation can be actually used to generate algorithms with PAC-MDP bounds. Investigating to what extent different auxiliary tasks impact the algorithm’s performance, and whether simpler tasks such as predicting feature activations or parts of the input (Jaderberg et al., 2017) are effective is also worth studying. Finally, it might be interesting to further investigate the connection between representation learning and exploration, since it is also known that better representations can lead to faster exploration (Jiang et al., 2017).

Acknowledgements

The authors would like to thank Jesse Farebrother for the initial implementation of DQN used in this paper, Georg Ostrovski for the discussions and for kindly providing us the exact results we report for DQN^{MMC}+CTS and DQN^{MMC}+PIXELCNN, and Yuri Burda for kindly providing us the data we used to compute the performance we report for RND in Atari 2600 games. We would also like to thank Carles Gelada, George Tucker and Or Sheffet for useful discussions, as well as the anonymous reviewers for their feedback. This work was supported by grants from Alberta Innovates Technology Futures and the Alberta Machine Intelligence Institute (Amii). Computing resources were provided by Compute Canada through CalculQuébec.

References

- Barreto, A., Dabney, W., Munos, R., Hunt, J., Schaul, T., Silver, D., and van Hasselt, H. Successor Features for Transfer in Reinforcement Learning. In *Advances in Neural Information Processing Systems (NIPS)*, pp. 4058–4068, 2017.
- Bellemare, M. G., Naddaf, Y., Veness, J., and Bowling, M. The Arcade Learning Environment: An Evaluation Platform for General Agents. *Journal of Artificial Intelligence Research*, 47:253–279, 2013.
- Bellemare, M. G., Srinivasan, S., Ostrovski, G., Schaul, T., Saxton, D., and Munos, R. Unifying Count-Based Exploration and Intrinsic Motivation. In *Advances in Neural Information Processing Systems (NIPS)*, pp. 1471–1479, 2016.
- Bellman, R. E. *Dynamic Programming*. Princeton University Press, Princeton, NJ, 1957.
- Brafman, R. I. and Tennenholtz, M. R-MAX - A General Polynomial Time Algorithm for Near-Optimal Reinforcement Learning. *Journal of Machine Learning Research*, 3:213–231, 2002.
- Burda, Y., Edwards, H., Storkey, A., and Klimov, O. Exploration by Random Network Distillation. In *Proceedings of the International Conference on Learning Representations (ICLR)*, 2019.
- Dayan, P. Improving Generalization for Temporal Difference Learning: The Successor Representation. *Neural Computation*, 5(4):613–624, 1993.
- Glorot, X. and Bengio, Y. Understanding the Difficulty of Training Deep Feedforward Neural Networks. In *Proceedings of the International Conference on Artificial Intelligence and Statistics (AISTATS)*, pp. 249–256, 2010.
- Jaderberg, M., Mnih, V., Czarnecki, W. M., Schaul, T., Leibo, J. Z., Silver, D., and Kavukcuoglu, K. Reinforcement Learning with Unsupervised Auxiliary Tasks. In *Proceedings of the International Conference on Learning Representations (ICLR)*, 2017.
- Jiang, N., Krishnamurthy, A., Agarwal, A., Langford, J., and Schapire, R. E. Contextual Decision Processes with Low Bellman Rank are PAC-Learnable. In *Proceedings of the International Conference on Machine Learning (ICML)*, pp. 1704–1713, 2017.
- Kearns, M. J. and Singh, S. P. Near-Optimal Reinforcement Learning in Polynomial Time. *Machine Learning*, 49(2-3):209–232, 2002.
- Kulkarni, T. D., Saeedi, A., Gautam, S., and Gershman, S. J. Deep Successor Reinforcement Learning. *CoRR*, abs/1606.02396, 2016.
- Machado, M. C., Bellemare, M. G., Talvitie, E., Veness, J., Hausknecht, M., and Bowling, M. Revisiting the Arcade Learning Environment: Evaluation Protocols and Open Problems for General Agents. *Journal of Artificial Intelligence Research*, 61:523–562, 2018a.
- Machado, M. C., Rosenbaum, C., Guo, X., Liu, M., Tesauro, G., and Campbell, M. Eigenoption Discovery through the Deep Successor Representation. In *Proceedings of the International Conference on Learning Representations (ICLR)*, 2018b.
- Martin, J., Sasikumar, S. N., Everitt, T., and Hutter, M. Count-Based Exploration in Feature Space for Reinforcement Learning. In *Proceedings of the International Joint Conference on Artificial Intelligence (IJCAI)*, pp. 2471–2478, 2017.
- Meyn, S. P. and Tweedie, R. L. *Markov Chains and Stochastic Stability*. 2012.
- Mnih, V., Kavukcuoglu, K., Silver, D., Rusu, A. A., Veness, J., Bellemare, M. G., Graves, A., Riedmiller, M., Fidjeland, A. K., Ostrovski, G., Petersen, S., Beattie, C., Sadik, A., Antonoglou, I., King, H., Kumaran, D., Wierstra, D., Legg, S., and Hassabis, D. Human-level Control through Deep Reinforcement Learning. *Nature*, 518:529–533, 2015.
- Oh, J., Guo, X., Lee, H., Lewis, R. L., and Singh, S. P. Action-Conditional Video Prediction using Deep Networks in Atari Games. In *Advances in Neural Information Processing Systems (NIPS)*, pp. 2863–2871, 2015.
- Osband, I., Roy, B. V., and Wen, Z. Generalization and Exploration via Randomized Value Functions. In *Proceedings of the International Conference on Machine Learning (ICML)*, pp. 2377–2386, 2016.

- Ostrovski, G., Bellemare, M. G., van den Oord, A., and Munos, R. Count-Based Exploration with Neural Density Models. In *Proceedings of the International Conference on Machine Learning (ICML)*, pp. 2721–2730, 2017.
- Plappert, M., Houthooft, R., Dhariwal, P., Sidor, S., Chen, R. Y., Chen, X., Asfour, T., Abbeel, P., and Andrychowicz, M. Parameter Space Noise for Exploration. In *Proceedings of the International Conference on Learning Representations (ICLR)*, 2018.
- Rummery, G. A. and Niranjan, M. On-line Q-Learning using Connectionist Systems. CUED/F-INFENG/TR 166, Cambridge University Engineering Dept., September 1994.
- Stadie, B. C., Levine, S., and Abbeel, P. Incentivizing Exploration in Reinforcement Learning With Deep Predictive Models. *CoRR*, abs/1507.00814, 2015.
- Strehl, A. L. and Littman, M. L. An Analysis of Model-based Interval Estimation for Markov Decision Processes. *Journal of Computer and System Sciences*, 74(8):1309–1331, 2008.
- Strehl, A. L., Li, L., Wiewiora, E., Langford, J., and Littman, M. L. PAC Model-Free Reinforcement Learning. In *Proceedings of the International Conference on Machine Learning (ICML)*, pp. 881–888, 2006.
- Sutton, R. S. Learning to Predict by the Methods of Temporal Differences. *Machine Learning*, 3:9–44, 1988.
- Tesauro, G. Temporal Difference Learning and TD-Gammon. *Communications of the ACM*, 38(3):58–68, 1995.
- Wu, Y., Tucker, G., and Nachum, O. The Laplacian in RL: Learning Representations with Efficient Approximations. In *Proceedings of the International Conference on Learning Representations (ICLR)*, 2019.

Supplemental Material: Count-Based Exploration with the Successor Representation

This document contains details omitted from the main text due to space constraints. The list of contents is below:

- Description of RiverSwim and SixArms, the tabular domains we used in our evaluation;
- Details about the methodology we used to evaluate Sarsa and Sarsa+SR;
- Pseudo-code for the model-based algorithm discussed in Section 3.2;
- Detailed description of the neural network implemented with $\text{DQN}_e^{\text{MMC}} + \text{SR}$;
- Learning curves for the experiments with DQN_e and $\text{DQN}_e^{\text{MMC}} + \text{SR}$ and the performance of these algorithms after different amounts of experience in the Atari 2600 games used in our evaluation;
- Learning curves for the experiments designed to evaluate the role of the auxiliary task in $\text{DQN}_e^{\text{MMC}} + \text{SR}$;
- Details about how we computed the performance of Random Network Distillation (RND);
- Learning curves and the performance after different amounts of experience of $\text{DQN}_e^{\text{MMC}} + \text{SR}$ when using the ℓ_1 -norm of the SR to generate the exploration bonus.

Description of RiverSwim and SixArms

The two domains we used as testbed to evaluate our ideas in the tabular case are shown in Figure 2. These domains are the same used by Strehl & Littman (2008). For SixArms, the agent starts in state 0. For RiverSwim, the agent starts in either state 1 or 2 with equal probability.

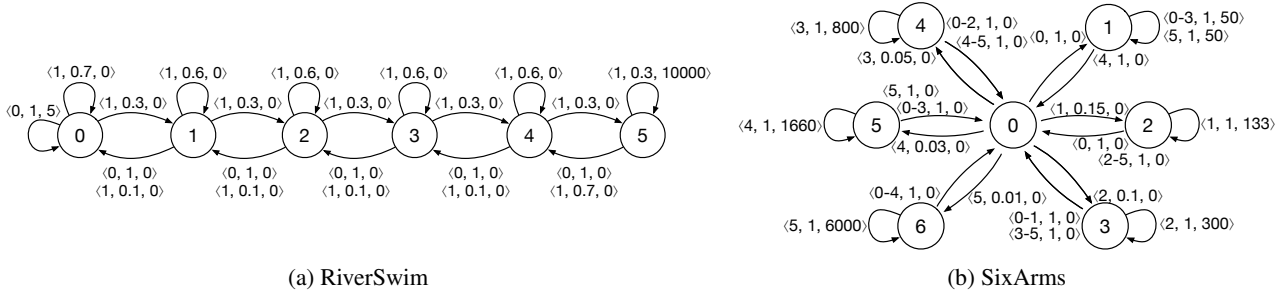


Figure 2. Domains used as testbed in the tabular case. The tuples in each transition should be read as $\langle \text{action id, probability, reward} \rangle$.

Methodology used to Evaluate Sarsa and Sarsa+SR

Both Sarsa and Sarsa+SR acted ϵ -greedily, maximizing the discounted return using $\gamma = 0.95$. For Sarsa+SR, we swept over different values of α , η , γ_{SR} , β and ϵ , with $\alpha \in \{0.01, 0.05, 0.1, 0.25, 0.5\}$, $\eta \in \{0.01, 0.05, 0.1, 0.25, 0.5\}$, $\gamma_{SR} \in \{0.5, 0.8, 0.95, 0.99\}$, $\beta \in \{1, 10, 100, 1000, 10000\}$ and $\epsilon \in \{0.01, 0.05, 0.1\}$. For Sarsa, we swept over the parameters α and ϵ . For fairness, we looked at a finer granularity for these parameters, with $\alpha \in i \times 0.005$ for i ranging from 1 to 100, and with $\epsilon \in j \times 0.01$ for j ranging from 1 to 15. Table 6 summarizes the parameter settings that led to the best results for each algorithm in RiverSwim and SixArms.

Algorithm	RiverSwim					SixArms				
	α	η	γ_{SR}	β	ϵ	α	η	γ_{SR}	β	ϵ
Sarsa	0.37	-	-	-	0.12	0.43	-	-	-	0.01
Sarsa+SR (w/ ℓ_1 -norm)	0.1	0.5	0.5	10,000	0.01	0.5	0.25	0.5	10,000	0.01
Sarsa+SR (w/ ℓ_2 -norm)	0.1	0.5	0.5	10,000	0.05	0.25	0.5	0.5	10,000	0.01

Table 6. Parameter settings that led to the reported performance in RiverSwim and SixArms.

Exploration through the Substochastic Successor Representation

In the main paper we described ESSR as a standard model-based algorithm where the agent updates its transition probability model and reward model through Equation 2 and its substochastic successor representation estimate as in Definition 3.1. The pseudo-code with details about the implementation is presented below.

Algorithm 1 Exploration through the Substochastic Successor Representation (ESSR)

```

 $n(s, s') \leftarrow 0 \quad \forall s, s' \in \mathcal{S}$ 
 $t(s, a, s') \leftarrow 1 \quad \forall s, s' \in \mathcal{S}, \forall a \in \mathcal{A}$ 
 $\hat{r}(s, a) \leftarrow 0 \quad \forall s \in \mathcal{S}, \forall a \in \mathcal{A}$ 
 $\hat{P}(s, a) \leftarrow 1/|\mathcal{S}| \quad \forall s \in \mathcal{S}, \forall a \in \mathcal{A}$ 
 $\tilde{P}(s, s') \leftarrow 0 \quad \forall s, s' \in \mathcal{S}$ 
 $\pi \leftarrow \text{random over } \mathcal{A}$ 
while episode is not over do
    Observe  $s \in \mathcal{S}$ , take action  $a \in \mathcal{A}$  selected according to  $\pi(s)$ , and observe a reward  $R$  and a next state  $s' \in \mathcal{S}$ 
     $n(s, s') \leftarrow n(s, s') + 1$ 
     $t(s, a, s') \leftarrow t(s, a, s') + 1$ 
     $n(s) \leftarrow \sum_{x', b} t(s, b, x')$ 
     $n(s, a) \leftarrow \sum_{x'} t(s, a, x')$ 
     $\hat{r}(s, a, s') \leftarrow \frac{(t(s, a, s') - 2) \times \hat{r}(s, a, s') + R}{t(s, a, s') - 1}$ 
    for each state  $x' \in \mathcal{S}$  do
         $\hat{P}(s, a, x') \leftarrow \frac{t(s, a, x')}{n(s, a)}$ 
         $\tilde{P}(s, x') \leftarrow \frac{n(s, x')}{n(s) + 1}$ 
    end for
     $\tilde{\Psi} \leftarrow (I - \gamma \tilde{P})^{-1}$ 
     $r_{\text{int}} \leftarrow -\tilde{\Psi} \mathbf{e}$ 
     $\pi \leftarrow \text{POLICYITERATION}(\hat{P}, \hat{r} + \beta r_{\text{int}})$ 
end while
    
```

Detailed Neural Network Architecture of $\text{DQN}_e^{\text{MMC}} + \text{SR}$

In order to allow the reader to focus on the general idea proposed in the paper, we decided to not present, in the main text, the detailed description of the architecture we used in $\text{DQN}_e^{\text{MMC}} + \text{SR}$. The detailed architecture is depicted in Figure 3, where we explicitly represent each layer and their parameters.

The loss functions and the optimizer used were described in the main paper. The only other important information is regarding the network’s initialization. We initialize our network the same way Oh et al. (2015) does. We use Xavier initialization (Glorot & Bengio, 2010) in all layers except the fully connected layers around the element-wise multiplication denoted by \otimes , which are initialized uniformly with values between -0.1 and 0.1 .

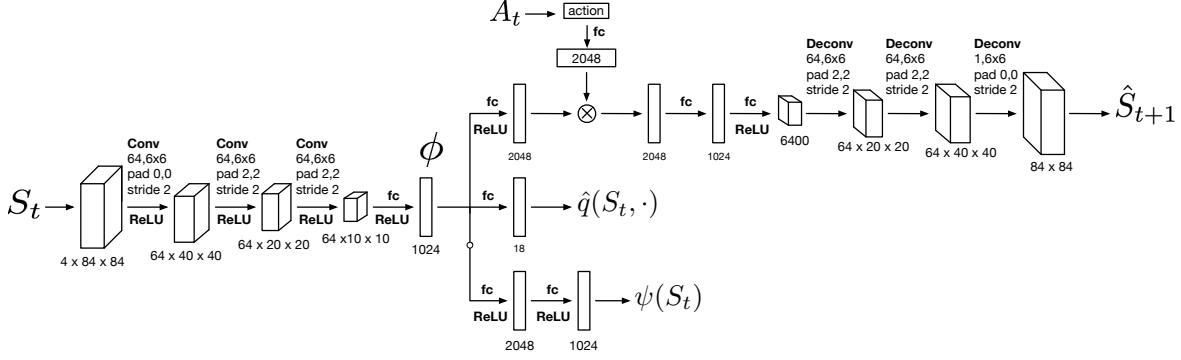


Figure 3. Neural network architecture used by our algorithm when learning to play Atari 2600 games.

Additional Results for $\text{DQN}_e^{\text{MMC}} + \text{SR}$ and $\text{DQN}_e^{\text{MMC}}$ in the Atari 2600 Games

As recommended by Machado et al. (2018a), we report the performance of $\text{DQN}_e^{\text{MMC}} + \text{SR}$ and $\text{DQN}_e^{\text{MMC}}$ after different amounts of experience (10, 50, and 100 million frames) in Tables 7 and 8.

Finally, Figure 4 depicts the learning curves obtained with the evaluated algorithms in each game. Lighter lines represent individual runs while the solid lines encode the average over the multiple runs.

Game	10M frames		50M frames		100M frames	
FREEWAY	24.9	(0.5)	29.5	(0.1)	29.5	(0.1)
GRAVITAR	244.1	(23.8)	326.4	(53.0)	430.3	(109.4)
MONT. REVENGE	2.6	(7.2)	563.8	(465.7)	1778.6	(903.6)
PRIVATE EYE	99.2	(1.2)	98.5	(3.3)	99.1	(1.8)
SOLARIS	1547.5	(410.9)	2036.3	(339.0)	2155.7	(398.3)
VENTURE	26.2	(22.1)	942.0	(423.8)	1241.8	(236.0)

 Table 7. Results obtained with $\text{DQN}_e^{\text{MMC}} + \text{SR}$ after different amounts of experience.

Game	10M frames		50M frames		100M frames	
FREEWAY	25.7	(1.5)	29.6	(0.1)	29.5	(0.1)
GRAVITAR	229.9	(31.3)	559.3	(75.9)	1078.3	(254.1)
MONT. REVENGE	0.0	(0.0)	0.0	(0.0)	0.0	(0.0)
PRIVATE EYE	216.7	(219.5)	109.1	(44.1)	113.4	(42.3)
SOLARIS	2230.0	(322.3)	2181.5	(292.9)	2244.6	(378.8)
VENTURE	63.8	(31.3)	794.1	(151.9)	1220.1	(51.0)

 Table 8. Results obtained with $\text{DQN}_e^{\text{MMC}}$ after different amounts of experience.

Evaluation of the Impact of the Auxiliary Task in $\text{DQN}_e^{\text{MMC}} + \text{SR}$

In the main paper we also evaluated whether the introduced *auxiliary task was necessary* and whether this *auxiliary task was sufficient* to obtain the performance reported for $\text{DQN}_e^{\text{MMC}} + \text{SR}$. The results suggest that while an auxiliary task is necessary for $\text{DQN}_e^{\text{MMC}} + \text{SR}$, it is definitely not sufficient to explain the obtained performance. This discussion is available in the main paper. Figure 5 depicts the learning curves for each individual run.

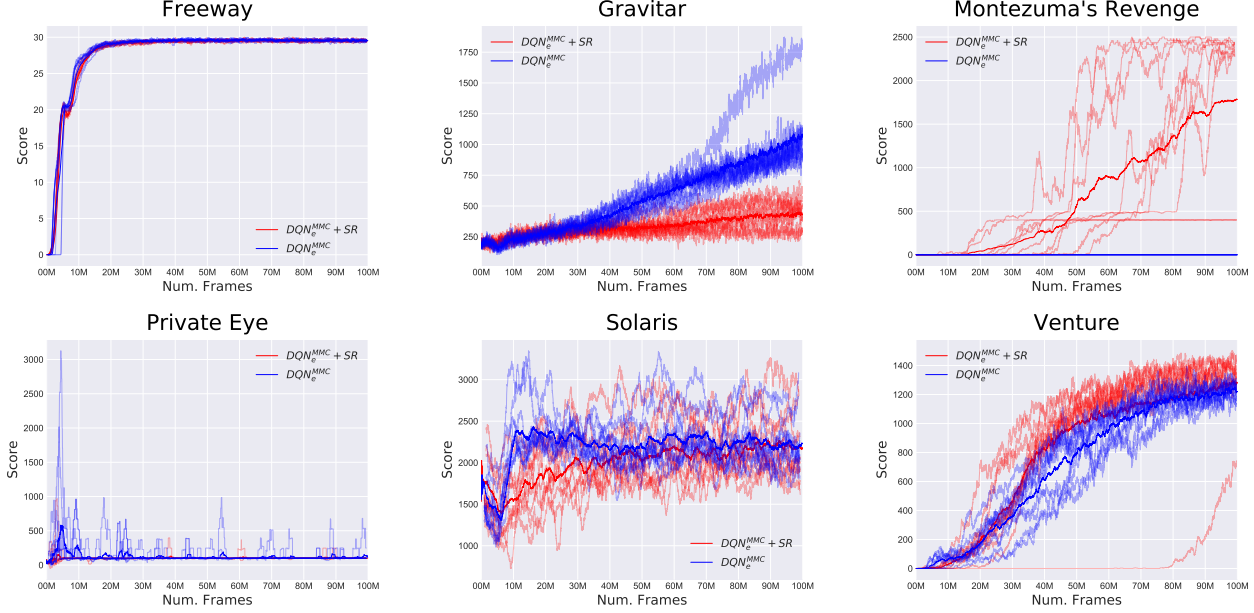


Figure 4. $DQN_e^{MMC}+SR$ and DQN_e^{MMC} learning curves in the Atari 2600 games used as testbed. The curves are smoothed with a running average computed using a window of size 100.

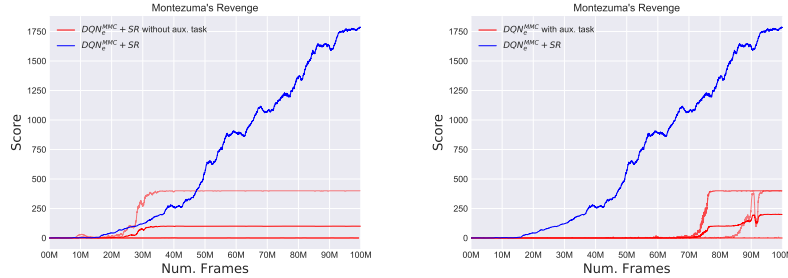


Figure 5. Evaluation of the impact of the auxiliary task in $DQN_e^{MMC}+SR$'s performance. The learning curves are smoothed with a running average computed using a window of size 100.

On the Reported Performance of Random Network Distillation (RND) in the ALE

We calculated the performance of RND from the data used by Burda et al. (2019) to plot Figure 7 of their paper. The authors shared this data with us. The performance we report is the average performance after 1,530 rollouts. Each rollout consists of 128 time steps with 4 frames per time step (128 environments were executed in parallel), leading to $1,530 \times 128 \times 128 \times 4 = 100,270,080$ frames. We averaged the performance over 3 seeds in the games GRAVITAR, PRIVATE EYE, SOLARIS, and VENTURE. The performance reported for MONTEZUMA'S REVENGE is the average over 10 seeds.

The Impact of Using the ℓ_1 and ℓ_2 -norm of the SR in $DQN_e^{MMC}+SR$

In the main paper we evaluated $DQN_e^{MMC}+SR$ using both the ℓ_1 - and ℓ_2 -norm of the SR. In this section we provide additional data related to $DQN_e^{MMC}+SR$ when using the ℓ_1 -norm of the SR. More specifically, Table 9 depicts the agent's performance after different amounts of experience while Figure 6 depicts the full learning curves. Finally, for completeness, Table 10 depicts the agent's performance after different amounts of experience for DQN_e^{MMC} when the feature representation is normalized with the ℓ_1 -norm instead of the ℓ_2 -norm of the SR.

Game	10M frames		50M frames		100M frames	
FREEWAY	23.5	(0.8)	29.3	(0.1)	29.4	(0.1)
GRAVITAR	238.8	(26.4)	343.0	(72.2)	457.4	(120.3)
MONT. REVENGE	0.2	(0.4)	591.3	(870.1)	1395.4	(1121.8)
PRIVATE EYE	97.2	(5.3)	99.4	(1.9)	104.4	(50.4)
SOLARIS	1455.7	(146.3)	1755.9	(237.5)	1890.1	(163.1)
VENTURE	29.0	(30.2)	1102.4	(77.6)	1348.5	(56.5)

Table 9. Results obtained with $DQN_e^{MMC}+SR$ after different amounts of experience when using the ℓ_1 -norm of the SR.

Game	10M frames		50M frames		100M frames	
FREEWAY	24.0	(8.4)	26.4	(9.3)	26.4	(9.3)
GRAVITAR	228.6	(26.9)	555.9	(35.6)	1063.1	(271.8)
MONT. REVENGE	0.1	(0.3)	0.6	(1.9)	40.0	(126.5)
PRIVATE EYE	97.3	(5.1)	102.8	(13.2)	98.7	(3.2)
SOLARIS	1873.6	(210.6)	2175.2	(243.8)	2028.7	(143.2)
VENTURE	48.1	(44.9)	795.3	(167.2)	1236.0	(51.3)

Table 10. Results obtained with DQN_e^{MMC} after different amounts of experience when using the ℓ_1 -norm in the normalization.

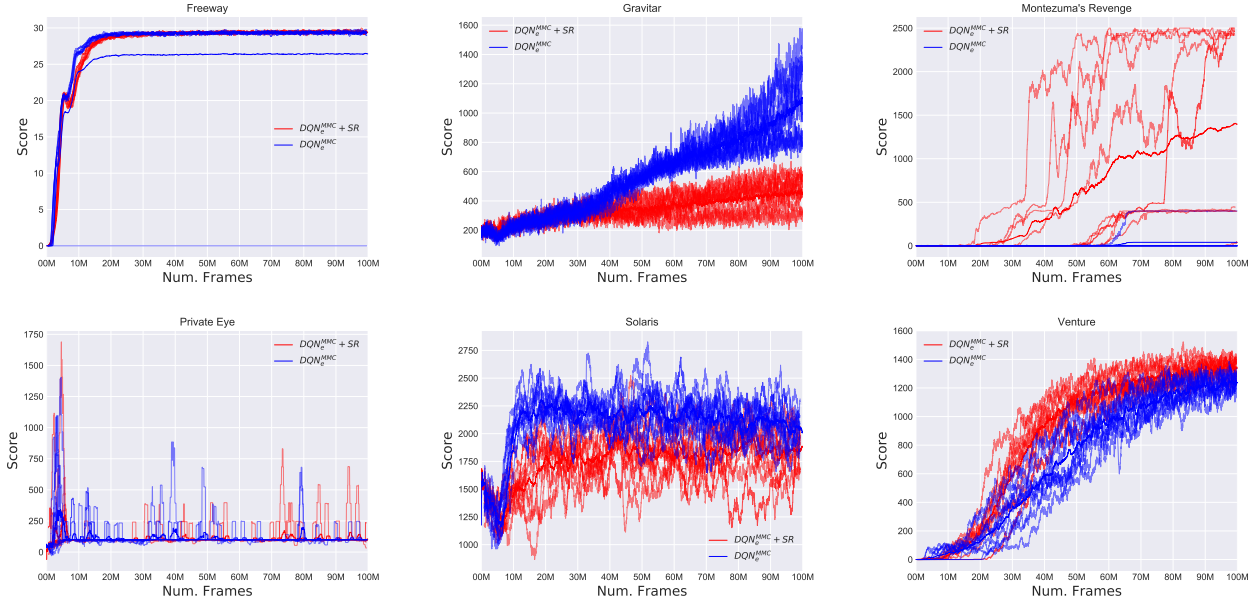


Figure 6. Learning curves for $DQN_e^{MMC}+SR$ and DQN_e^{MMC} , when using the ℓ_1 -norm of the SR, in the Atari 2600 games used as testbed. The curves are smoothed with a running average computed using a window of size 100.